Sodium-Calcium Exchange Is Essential for Effective Triggering of Calcium Release in Mouse Heart

Patricia Neco,[†] Beth Rose,[†] Nhi Huynh,[†] Rui Zhang,[†] John H. B. Bridge,[‡] Kenneth D. Philipson,[†] and Joshua I. Goldhaber[†*]

[†]Departments of Medicine (Cardiology) and Physiology and the Cardiovascular Research Laboratories, David Geffen School of Medicine at UCLA, Los Angeles, California; and [‡]Cardiovascular Research Training Institute, University of Utah, Salt Lake City, Utah

ABSTRACT In cardiac myocytes, excitation-contraction coupling depends upon sarcoplasmic reticular Ca^{2+} release triggered by Ca^{2+} influx through L-type Ca^{2+} channels. Although Na^{+}-Ca^{2+} exchange (NCX) is essential for Ca^{2+} extrusion, its participation in the trigger process of excitation-contraction coupling is controversial. To investigate the role of NCX in triggering, we examined Ca^{2+} sparks in ventricular cardiomyocytes isolated from wild-type (WT) and cardiac-specific NCX knockout (KO) mice. Myocytes from young NCX KO mice are known to exhibit normal resting cytosolic Ca^{2+} and normal Ca^{2+} transients despite reduced L-type Ca^{2+} current. We loaded myocytes with fluo-3 to image Ca^{2+} sparks using confocal microscopy in line-scan mode. The frequency of spontaneous Ca^{2+} sparks was reduced in KO myocytes compared with WT. However, spark amplitude and width were increased in KO mice. Permeabilizing the myocytes with saponin eliminated differences between spontaneous sparks in WT and KO mice. These results suggest that sarcolemmal processes are responsible for the reduced spark frequency and increased spark width and amplitude in KO mice. When myocytes were loaded with 1 mM fluo-3 and 3 mM EGTA via the patch pipette to buffer diadic cleft Ca^{2+}, the number of sparks triggered by action potentials was reduced by 60% in KO cells compared to WT cells, despite similar SR Ca^{2+} content in both cell types. When EGTA was omitted from the pipette solution, the number of sparks triggered in KO and WT myocytes was similar. Although the number of sparks was restored in KO cells, Ca^{2+} release was asynchronous. These results suggest that high subsarcolemmal Ca^{2+} is required to ensure synchronous triggering with short spark latency in the absence of NCX. In WT mice, high subsarcolemmal Ca^{2+} is not required for synchronous triggering, because NCX is capable of priming the diadic cleft with sufficient Ca^{2+} for normal triggering, even when subsarcolemmal Ca^{2+} is lowered by EGTA. Thus, reducing subsarcolemmal Ca^{2+} with EGTA in NCX KO mice reveals the dependence of Ca^{2+} release on NCX.

INTRODUCTION

In cardiac myocytes, depolarization by action potentials (APs) elicits Ca^{2+} influx through L-type Ca^{2+} channels (LCCs), which in turn triggers Ca^{2+} release from ryanodine receptors (RyRs) located on the terminal cisternae of the junctional sarcoplasmic reticulum (SR). This Ca^{2+}-induced Ca^{2+}-release mechanism (1) is localized to diadic clefts at junctions of the SR and the sarcolemma along transverse tubules (t-tubules) of ventricular myocytes. Ca^{2+} must diffuse across the diadic cleft from the LCCs in the sarcolemma to the RyRs on the SR membrane (2–4). SR Ca^{2+} released into the cleft by RyRs can be detected as Ca^{2+} sparks using laser scanning confocal microscopy (5). The recruitment of large numbers of Ca^{2+} sparks during an AP produces the cytosolic Ca^{2+} transient (6). In the steady state, Ca^{2+} entry into the cell must be balanced by Ca^{2+} efflux, which occurs by Na^{+}-Ca^{2+} exchange (NCX), the dominant Ca^{2+} efflux mechanism in cardiac cells. Although NCX is thought of first and foremost as a Ca^{2+} extrusion mechanism, it has been proposed that the exchanger may operate in reverse mode as an alternate or second source of trigger Ca^{2+} (7–10). During an AP, the combination of depolarization and accumulation of Na^{+} near the membrane may favor reversal of NCX and hence Ca^{2+} entry (8,11). Leblanc and Hume (7) proposed that the inward Na^{+} current (I_{Na}) was capable of producing an increase in subsarcolemmal Na^{+} sufficient to reverse NCX and thereby raise cytoplasmic Ca^{2+} to the point where NCX could trigger SR Ca^{2+} release. This finding has remained largely unsubstantiated, because follow-up studies suggested that Ca^{2+} entry via reverse NCX was 1), too slow, 2), too brief, and 3), too small to trigger Ca^{2+} release under physiological conditions (12–14). The finding that NCX may be located among LCCs (15) has renewed interest in the possible contribution of NCX to triggering, since its close proximity to RyRs might facilitate interaction between the two.

We have generated ventricular-specific NCX knockout (KO) mice using cre/lox technology (16). These mice have minimal cardiac dysfunction through young adulthood. NCX KO mice do not upregulate alternative Ca^{2+} extrusion mechanisms and therefore have severely impaired Ca^{2+} efflux capacity. To compensate for the absence of NCX, KO mice limit Ca^{2+} entry by abbreviating the AP (17) and reducing the L-type Ca^{2+} current (I_{Ca}) (18). Despite the reduction in I_{Ca}, SR Ca^{2+} release is maintained at wild-type (WT) levels. This may be due in part to rapid repolarization of the KO AP, attributable to increased

Submitted August 28, 2009, and accepted for publication April 30, 2010.

*Correspondence: jgoldhaber@mednet.ucla.edu

Editor: Michael D. Stern.

0006-3495/10/08/0755/10 $2.00

doi: 10.1016/j.bpj.2010.04.071

transient outward current (I_{to}) (19). Thus, in KO myocytes, there is decreased transsarcolemmal Ca^{2+} flux without compromised contractility (16,19). NCX KO mice enable us to further examine the contribution of NCX to excitation-contraction (EC) coupling in heart.

The aim of this study is to investigate how NCX influences the activity of resting and triggered Ca^{2+} sparks. We used laser scanning confocal microscopy and fluo-3 to study resting Ca^{2+} sparks in intact and permeabilized mouse cardiomyocytes, as well as Ca^{2+} sparks triggered by APs in both WT and cardiac-specific NCX KO myocytes. Our results suggest that NCX ensures normal triggering of Ca^{2+} release in WT mice by priming the diadic cleft with Ca^{2+} upon depolarization.

MATERIALS AND METHODS

Our experiments were conducted on ventricular myocytes isolated enzymatically from WT and cardiac-specific NCX KO mice (16). We measured sparks in both intact cells (20) at rest and cells permeabilized with the detergent saponin (21). In other experiments, we simultaneously recorded membrane potential and evoked Ca^{2+} sparks with APs. To accomplish this, patch-clamped ventricular myocytes were loaded via the patch pipette with fluo-3 (1 mM), with or without the addition of EGTA (3 mM), and then imaged using the ultrarapid line-scan mode (0.24 ms/line) of a Noran Odyssey XL laser scanning confocal microscope (22). A complete description of the methods can be found in the Supporting Material.

RESULTS

Spontaneous Ca^{2+} spark frequency is reduced in NCX KO myocytes

We have established that calcium efflux in NCX KO mice is reduced compared to that in WT mice (19). To determine whether this reduced efflux influences spark properties such as size, we measured the characteristics of spontaneous sparks in patch-clamped mouse ventricular myocytes loaded with the Ca^{2+} indicator fluo-3, held at a constant potential of −75 mV, and imaged with laser scanning confocal microscopy in line-scan mode (2 ms/line) (22). Spark amplitude and width (full width at half-maximum (FWHM)) were larger in KO than WT mice (Fig. 1, *B* and *C*), but spark frequency was lower in KO mice. This is evident in the representative line-scan images shown in Fig. 1 *A*, where seven sparks are visible in the WT image but only three can be seen in the KO image. Spark amplitude depends upon the flux of Ca^{2+} released from clusters of RyRs in a couplon and the rate at which this Ca^{2+} is removed from the vicinity of the couplon by diffusion, SR uptake by SERCA, and transsarcolemmal efflux by the plasma membrane Ca^{2+} pump and NCX. Since NCX is absent in KO mice, efflux is slow (19), and thus sufficient to explain the higher spark amplitude. The reduced frequency of resting sparks in KO myocytes could either be caused by altered triggers (e.g., lack of NCX or altered LCCs) or by altered release mechanisms (e.g., RyRs or SR Ca^{2+}). We

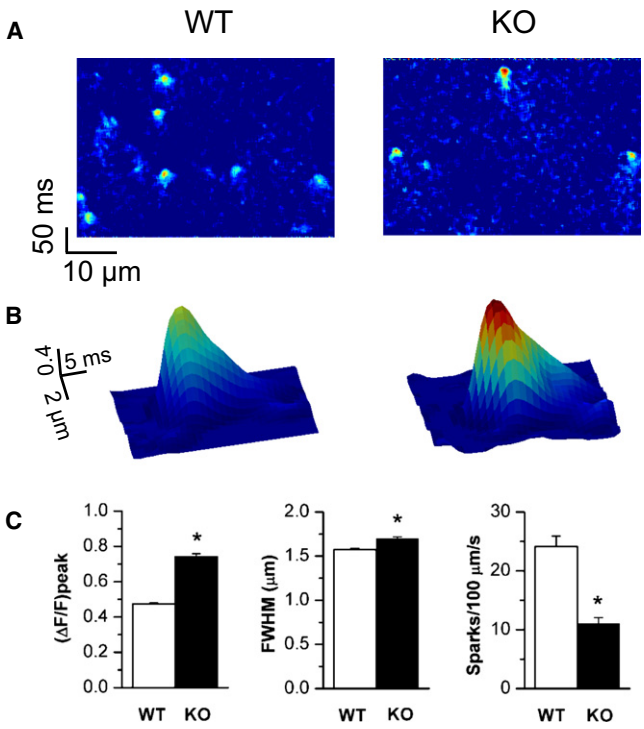

FIGURE 1 Ca^{2+} sparks in resting WT and NCX KO myocytes. (*A*) Confocal line-scan images (2 ms/line) recorded in quiescent WT (*left*) and KO (*right*) mouse ventricular myocytes loaded with fluo-3 AM. Note the decreased number of sparks in the KO image. (*B*) 3D plots on a spatio-temporal scale showing representative Ca^{2+} sparks recorded in WT (*left*) and KO (*right*) cells. (*C*) Mean spark amplitude (ΔF/F), FWHM, and frequency observed in quiescent WT (*white bars*, $n = 10$ cells from three WT mice) and NCX KO (*black bars*, $n = 8$ cells from four KO mice) myocytes. $^*P < 0.05$.

have demonstrated previously that there is a 50% reduction in I_{Ca} in KO cells (16,18). This reduction in I_{Ca} is caused by accumulation of subsarcolemmal Ca^{2+}, which increases Ca^{2+}-dependent inactivation of LCCs (18). Since our previous studies have shown that SR Ca^{2+} content is identical in WT and KO cells (19), the reduction in I_{Ca} is a leading candidate for the lower spark frequency in KO cells.

To examine the influence of the sarcolemma on resting Ca^{2+} sparks, we compared spark characteristics in resting WT and KO ventricular myocytes permeabilized with the detergent saponin and loaded with fluo-3. Permeabilization mitigates the influence of sarcolemmal processes on RyRs, and exposes the RyRs from both WT and KO cells to exactly the same cytoplasmic Ca^{2+} concentration. We found that sparks from WT and KO cells were indistinguishable after permeabilization with regard to amplitude, duration, and frequency (Fig. 2). These data suggest that sarcolemmal processes regulating diadic cleft Ca^{2+}, rather than compensatory changes in RyR activity or SR Ca^{2+}, are primarily responsible for the differences in WT and KO Ca^{2+} spark properties.

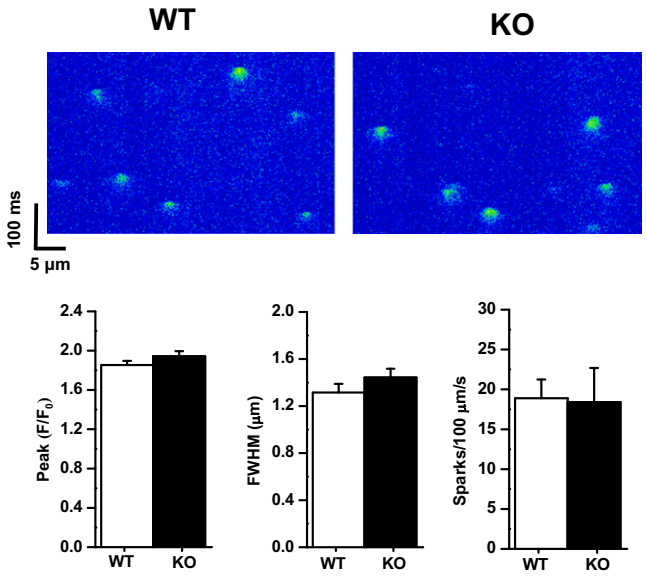

FIGURE 2 Ca^{2+} sparks in permeabilized WT and NCX KO myocytes. Confocal line-scan images (2 ms/line) of Ca^{2+} sparks recorded in representative WT (*upper left*) and KO myocytes (*upper right*) permeabilized with saponin and loaded with fluo-3 (resting free Ca^{2+} set to 60 nM). The bar graphs below show no difference in peak fluorescence (F/F_0), size (FWHM), or frequency of sparks (mean + SE) in seven cells from two WT mice, and seven cells from two KO mice. We obtained similar results in 25 WT and KO cells from three WT and three KO mice in which the resting Ca^{2+} was set to 100 nM (data not shown).

Action potential-evoked Ca^{2+} sparks in NCX KO myocytes

We next investigated sparks evoked by APs in WT and NCX KO myocytes. We have observed previously that Ca^{2+} transients in WT and KO cells are similar (16,19), despite a smaller I_{Ca} in the KO mice. Thus, EC coupling gain (defined as the ratio of Ca^{2+} release to the magnitude of I_{Ca}) is significantly higher in KO mice. Since there is no evidence of enlarged SR Ca^{2+} content in KO myocytes, we propose that coupling fidelity, i.e., the fraction of single LCC openings that successfully trigger sparks (23), is higher in KO than in WT myocytes. This would enable a reduced trigger within a KO couplon to match the probability of spark activation in the WT (with its larger trigger), accounting for the increased gain. We hypothesize that the elevated Ca^{2+} concentration in the diadic cleft of KO myocytes due to reduced Ca^{2+} efflux (18) accounts for the higher coupling fidelity and gain. Elevated cleft Ca^{2+} should increase the probability that an LCC opening triggers Ca^{2+} release, because further Ca^{2+} loading, or priming, of the diadic cleft by NCX is not required. In WT cells, which have a lower cleft Ca^{2+} concentration to begin with, NCX can help prime the diadic cleft before activation by LCCs and therefore increase coupling fidelity (8).

We investigated this possibility by studying Ca^{2+} spark formation using high-speed line-scan confocal imaging during APs in WT and KO myocytes. EGTA (3 mM) was included in the pipette solution along with 1.3 mM Ca^{2+} to set free Ca^{2+} at 100 nM. EGTA is often used in confocal imaging to investigate the spatiotemporal characteristics of Ca^{2+}-dependent phenomena (22,24–27), because it constrains visualization of Ca^{2+} to the source of release, and the peak of the resulting spike measures the flux of Ca^{2+} from a couplon (28). In these experiments, we also used EGTA to lower diadic cleft Ca^{2+} to expose the intrinsic effectiveness of I_{Ca} in activating a couplon. For convenience, we will continue to refer to local Ca^{2+} release under these highly buffered conditions as sparks.

When EGTA was included in the pipette, APs activated more Ca^{2+} release sites in WT cells than in KO cells. In a representative WT myocyte, an AP evoked 20 Ca^{2+} release events (Fig. 3 *left*). In contrast, only 11 Ca^{2+} release events were evoked in a typical KO myocyte (Fig. 3 *right*). NCX KO myocytes exhibited a greater number of regions where Ca^{2+} release events were not evoked by APs along the scan line, i.e., fluorescence values were close to background. These are seen clearly when the timescale is expanded (Fig. 3 *B*, *arrowheads*). Locations where sparks are absent in KO myocytes indicate a total failure of couplon activation. These temporally silent regions were observed in all NCX KO myocytes equilibrated with 3 mM EGTA. In summary, there were a total of 135 Ca^{2+} release events in eight WT cells (17 ± 1/cell) but only 56 Ca release events in eight KO cells (7 ± 1/cell, $P < 0.0001$).

We also found a significant difference in the latency of Ca^{2+} release events between WT and KO myocytes. In WT cells, all Ca^{2+} release events occurred within 15 ms of the AP stimulus (Fig. 3 *C*, *left*), whereas in KO cells, spark activation latencies were distributed throughout the recording period (Fig. 3 *C*, *right*). In both cases, examination of the line-scan images and their corresponding APs on an expanded timescale (scale bar, 10 ms) show that the leading edge of the Ca^{2+} transient begins just after the onset of the repolarization phase of the AP (*dashed lines*). Only 77% of release events occurred within 15 ms of the AP stimulus in KO cells compared with 100% in WT (Fig. 3 *C*). We termed this group of Ca^{2+} sparks the early pool, because they appeared proximate to the AP depolarization. We termed the other 23% of sparks that occurred after the initial 15 ms the late pool. The average latency of the early pool was (in ms) 2.4 ± 0.2 for WT and 2.7 ± 0.3 for KO ($P = 0.3$; see Fig. 5 *B*), whereas the average latency (including both pools) was (in ms) 2.4 ± 0.2 for WT and 21.0 ± 2.0 for KO ($P < 0.0001$; see Fig. 5 *A*). Thus, in NCX KO myocytes, AP-evoked Ca^{2+} spark triggering in the presence of EGTA was both reduced and poorly synchronized compared to that in WT myocytes. Rapid caffeine application (5 mM) revealed no reduction in SR Ca content in KO compared to WT myocytes that might account for these changes ($\Delta F/F_0$ of 1.7 ± 0.1 in WT and 1.8 ± 0.2 in KO myocytes, $P = 0.73$). We suggest that loss of NCX prevents normal activation of couplons when EGTA is

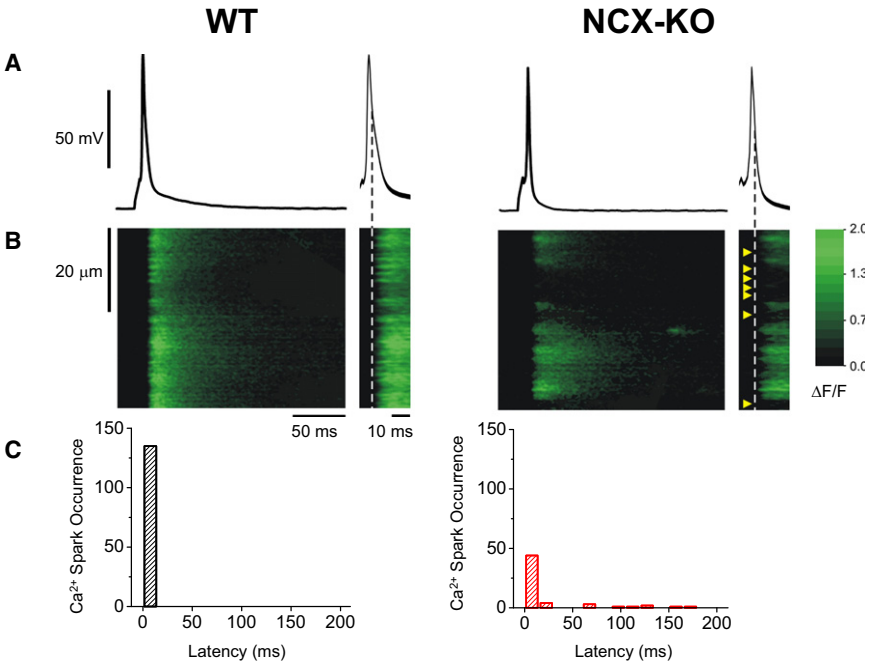

FIGURE 3 Ca^{2+} sparks evoked by APs in WT and NCX KO myocytes in the presence of 3 mM EGTA. (*A*) Representative APs stimulated by current commands and (*B*) corresponding rapid (0.24 ms/line) line-scan images recorded simultaneously in representative WT and NCX KO myocytes. Cells were loaded with 1 mM fluo-3 and 3 mM EGTA via the patch pipette. APs and images are also shown on a higher-resolution temporal scale (scale bar, 10 ms). Dashed line indicates the time when the earliest Ca^{2+} spark was activated. Arrowheads mark the positions where couplons failed to activate. Fluorescence intensities are reported in self-ratioed ΔF/F magnitude as indicated in the adjoining palette. (*C*) Ca^{2+} spark latency histograms (15-ms bins) constructed from line-scan images recorded in WT (*left*, $n = 8$ cells from four mice) and NCX KO (*right*, $n = 8$ cells from four mice) myocytes.

present to buffer Ca^{2+} and prevent priming of the diadic cleft. Under these conditions, we speculate that coupling fidelity is less in KO than in WT, where priming of the diadic cleft may still occur via reverse NCX in response to activation of I_{Na} and depolarization.

Improved EC coupling in NCX KO myocytes in the absence of EGTA

We further investigated coupling fidelity by repeating the above experiments without EGTA in the pipette. Fluo-3 was still present at 1 mM to help resolve Ca^{2+} sparks during the high-speed line scan. In the absence of pipette EGTA (Fig. 4), there was no difference in the total number of evoked sparks in WT and KO cells, though the distribution of spark latencies remained different between the two cell types. Fig. 4 shows the temporal relationship between APs (*A*) and Ca^{2+} release (*B*) in representative WT and NCX KO myocytes patch-clamped in the absence of EGTA. The line-scan image in the left panel of Fig. 4 *B*, recorded from a WT cell, exhibits activation of 19 Ca^{2+} release sites recorded from a 41-μm-wide region of a cell. These release sites are clearly triggered in a synchronous fashion with a very short latency of 1.8 ± 0.2 ms. The AP duration at 90% repolarization was 24 ms.

The line-scan image in Fig. 4 *B* (*right*), recorded from an NCX KO myocyte, shows a total of 18 evoked Ca^{2+} release sites, similar to WT myocytes. However, unlike WT myocytes, only 14 of these were triggered at the beginning of the Ca^{2+} transient. The latency of these early sparks was 2.2 ± 0.1 ms. The other four Ca^{2+} sparks were triggered 15, 84, 112, and 140 ms after the AP peak, raising the total averaged Ca^{2+} spark latency to 21.3 ± 10.4 ms in this cell. The expanded timescale in Fig. 4 *B*, *right* (scale bar, 10 ms) shows that, similar to WT, the leading edge of the Ca^{2+} transient starts during the repolarization phase of the AP. However, as with the high-EGTA group, fewer sparks were observed at the onset of the transient. Once again, there were temporally silent locations in the KO cells where AP-evoked Ca^{2+} release sites were absent or substantially delayed (Fig. 4 *B*, *arrowheads*).

These findings were typical of our observations in all cells studied when EGTA was omitted from the pipette solution. Overall a similar number of sparks was triggered in both WT and KO cells during the total 230-ms recording period (17 ± 2 and 16 ± 2, respectively; $n = 8$ in each group; $P = 0.8$). However, the latency of activation differed considerably between the two groups. Frequency histograms of Ca^{2+} spark latencies for eight WT and eight KO cells (Fig. 4 *C*) show that in WT cells, 100% of sparks ($N = 133$) were evoked within the first 15 ms of the AP (highly synchronized), whereas spark occurrence was broadly distributed (poorly synchronized) in KO cells. Only 66% ($N = 81$) of sparks from KO cells occurred within 15 ms of the AP (early pool), whereas 34% ($N = 43$) occurred later. The average latency of the early pool was (in ms) 1.9 ± 0.2 for WT and 2.2 ± 0.2 for KO ($P = 0.26$; Fig. 5 *B*), but when considering both pools, the average latency was (in ms) 1.9 ± 0.2 for WT and 33.4 ± 6.6 for KO ($P < 0.001$; Fig. 5 *A*). Thus, omitting EGTA restored the number of triggered calcium sparks in KO cells to WT cell levels, but did not reduce the latency of these Ca^{2+} release events in KO cells to WT values, as shown in Fig. 5. It is noteworthy that in these experiments we used

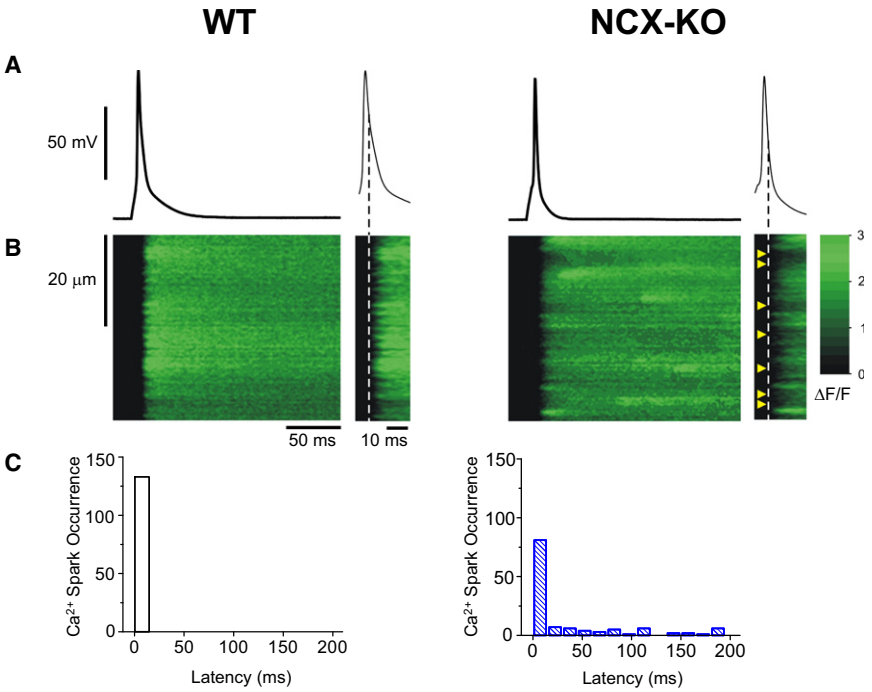

FIGURE 4 Ca^{2+} sparks evoked by APs in WT and NCX KO ventricular myocytes in the absence of EGTA. Representative APs stimulated by current commands (*A*) and corresponding rapid (0.24 ms/line) line-scan images (*B*) recorded simultaneously in representative WT and NCX KO myocytes loaded with 1 mM fluo-3 (but no EGTA) via the patch pipette. APs and images are also shown on a higher-resolution temporal scale (scale bar, 10 ms). Dashed line indicates the time when the earliest Ca^{2+} spark was activated. Arrowheads mark the positions on the line-scan images where couplons failed to activate. Fluorescence intensities are reported in self-ratioed ΔF/F magnitude as illustrated in the adjoining palette. (*C*) Ca^{2+} spark latency histograms (15-ms bins) constructed from line-scan images recorded in WT (*left*, $n = 8$ cells from four mice) and NCX KO (*right*, $n = 8$ cells from four mice) myocytes.

a high concentration of fluo-3 so that we could reliably image the local release events. Therefore, even though we removed EGTA, we did not completely eliminate Ca^{2+} buffering. Nevertheless, the results are consistent with the idea that Ca^{2+} in the diadic cleft of KO cells influences their coupling fidelity and hence the number of initial release events. These changes were not caused by decreased SR content, which was the same in the two groups ($\Delta F/F_0 = 4.0 \pm 0.7$ in WT and 4.4 ± 1.0 in KO cells, $P = 0.63$). We will address the issue of delayed sparks and increased latencies in the Discussion section. Finally, we reported previously that Ca^{2+} transients in KO and WT cells are identical (16,19). This is under circumstances where there is no buffering by EGTA and where the concentration of Ca^{2+} indicator is low to avoid Ca^{2+} buffering, in contrast to the experiments described here, where we deliberately buffered Ca^{2+}.

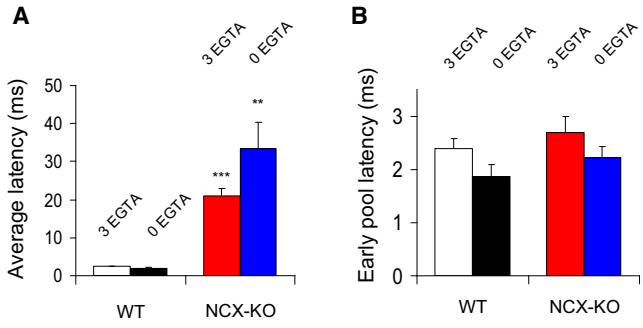

FIGURE 5 Latency of Ca^{2+} sparks evoked by APs in WT and KO myocytes Bar plots showing the mean latency of Ca^{2+} sparks identified during the 230-ms recording period. Confocal line scans (at 0.24 ms/line) were obtained as shown in Figs. 3 and 4 in WT and NCX KO myocytes. (*A*) shows averaged latencies for WT and KO myocytes buffered with 3 and 0 mM EGTA (via the patch pipette), respectively. (*B*) Latencies of sparks during the first 15 ms after the stimulus (early pool) obtained for the same conditions indicated in *A*. Regardless of the EGTA concentration, there was a significant increase in average latency in the NCX KO compared with WT mice (**$P < 0.001$ for KO versus WT in 0 mM EGTA and ***$P < 0.0001$ for KO versus WT in 3 mM EGTA), but only a trend toward increased latency of either cell type alone in 3 mM EGTA vs. 0 mM EGTA.

Effect of EGTA on the spatially averaged Ca^{2+} transient

The reduction in Ca^{2+} release events in KO cells loaded with EGTA should result in a reduction in the spatially averaged Ca^{2+} transient compared with WT. To demonstrate this, we measured spatially averaged fluorescence transients from line scans recorded in the presence and absence of EGTA. Fig. 6 *A* shows superimposed traces of the evoked Ca^{2+} transient recorded from representative WT and KO myocytes loaded with 1 mM fluo-3 and 3 mM EGTA. In both cases, there was a rapid rise of the transient, as seen in the normalized traces (Fig. 6 *A*, *inset*). Consistent with the reduced spark activation, the KO trace did not reach as high a peak as that seen in the WT trace. On average, peak fluorescence in KO myocytes was reduced 62% compared to WT myocytes ($\Delta F/F_0 = 1.02 \pm 0.12$ for WT and 0.40 ± 0.15 for KO myocytes, $P < 0.001$; Fig. 6 *B*). Both transients decayed quickly to baseline after the peak, consistent with EGTA reducing the diffusion of bound dye (29). However, the KO transients decayed more slowly than the WT transients ($\tau = 48 \pm 3$ ms for KO and 37 ± 2 for WT transients, $P < 0.05$), most likely because the lack of NCX reduces efflux rate.

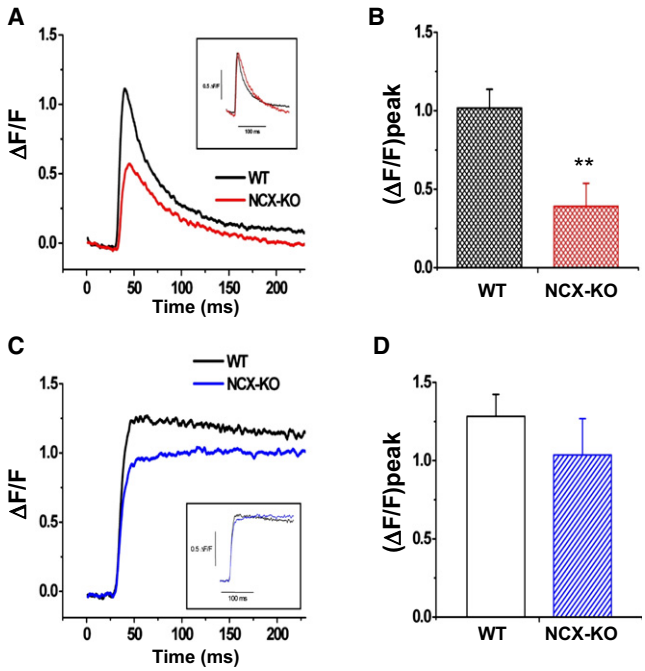

FIGURE 6 Spatially averaged Ca^{2+} transients in WT and NCX KO myocytes. (*A* and *C*) Superimposed AP-evoked Ca^{2+} transients obtained from representative WT and KO myocytes loaded with 1 mM fluo-3 and 3 mM EGTA (*A*) or 1 mM fluo-3 without added EGTA (*C*). (*Insets*) The same Ca^{2+} transients normalized to peak to illustrate the decay. (*B* and *D*) Bar plots show the peak ΔF/F of the spatially averaged Ca^{2+} transients recorded in WT ($N = 8$) and KO ($N = 8$) myocytes loaded with 1 mM fluo-3 and 3 mM EGTA (*B*) or 1 mM fluo-3 alone (*D*). $^{**}P < 0.001$ for KO versus WT.

In the complete absence of EGTA, differences in the fluorescence transients between WT and KO transients were less apparent. Transients from representative WT and KO cells are shown in Fig. 6 *C*. Both WT and KO have an initial rapid rising phase, followed by a very slow decay in the WT and a continued slow rise in the KO. Pooled data from multiple experiments ($N = 8$ for each condition) show that there is no significant reduction in peak fluorescence in KO ($\Delta F/F_0 = 1.04 \pm 0.23$) compared with WT transients ($\Delta F/F_0 = 1.28 \pm 0.14$; $P = 0.4$; Fig. 6 *D*). Transients decline very slowly in both cases, an expected consequence of the high concentration of fluo-3 in the cell (30).

T-tubular system remains normal in NCX KO myocytes

A disruption of the t-tubule system has been implicated in the pathogenesis of asynchronous SR Ca^{2+} release in models of heart failure (31–33). To investigate whether t-tubule spatial remodeling could explain the increased dispersion of latencies in KO myocytes, we examined the t-tubule network in isolated WT and KO cells using the potentiometric dye di-8 ANEPPS and 2-D confocal microscopy (27,33). We found that both WT and KO cells exhibited the classical striated pattern of t-tubule distribution. Plots of fluorescence intensity profiles along the long axis of these cells revealed a peak and valley distribution that was comparable in WT and KO cells. This suggests that the t-tubule network is preserved in cells lacking NCX. Average sarcomere lengths estimated from Gaussian fits to the fluorescence profiles were similar in both groups of cells (1.81 ± 0.02 and 1.79 ± 0.02 μm for WT ($N = 7$) and KO ($N = 10$), respectively). T-tubule densities were also similar ($25.7 \pm 0.7\%$ for WT and $25.0 \pm 0.9\%$ for KO). Thus, there is no alteration in the 2-D appearance of the t-tubular network morphology in KO myocytes. Representative images and fluorescence profiles can be viewed in Fig. S1 in the Supporting Material.

DISCUSSION

NCX KO mice live into young adulthood with remarkably well preserved cardiac function. Ca^{2+} transients in ventricular myocytes isolated from these mice are indistinguishable from those found in WT myocytes when recorded with conventional fura-2 epifluorescence photometry (19). However, laser scanning confocal microscopy reveals several differences in the individual Ca^{2+} sparks whose sum comprises the spatially averaged Ca^{2+} transient. Although resting Ca^{2+} sparks from KO mice are brighter and larger than those from WT mice, resting spark frequency is reduced in KO compared to WT mice. In addition, AP-evoked Ca^{2+} sparks in KO myocytes loaded with 1 mM fluo-3 are poorly synchronized compared to WT myocytes, with late sparks occurring well after repolarization is complete. The addition of EGTA to more strongly buffer subsarcolemmal Ca^{2+} further interferes with spark recruitment in KO myocytes, though EGTA has no such effect in WT. These differences in spark characteristics suggest a requirement for diadic cleft priming by NCX in normal EC coupling.

Ca^{2+} sparks in resting myocytes from WT and NCX KO mice

We find that knocking out NCX results in brighter and larger spontaneous sparks in unstimulated patch-clamped myocytes held at a resting potential of −75 mV. In addition, the frequency of spontaneous sparks is lower in KO than in WT mice. There are two broad possible explanations for these differences: 1), the properties of the SR are modified in the KO mice—for example, the open-time distribution of RyRs is decreased or the SR is depleted of Ca^{2+}; or 2), some process integral to the sarcolemmal membrane affects spontaneous spark properties. For this reason, we investigated spontaneous sparks after permeabilizing WT and KO myocytes with saponin to mitigate the influence of the sarcolemma while retaining the influences of RyR, SERCA, and SR Ca^{2+}. Permeabilization eliminated all

differences in resting spark properties. We conclude that the differences in spontaneous spark properties in WT and KO mice are attributable to changes in some sarcolemmal process. There are two processes associated with the sarcolemmal membrane that could influence resting spark production; these include 1), spontaneous LCC activity, and 2), NCX activity. At the moment, we cannot distinguish between these processes. However, it seems plausible that if the reason for a reduced I_{Ca} in KO myocytes (18) is a reduction in LCC open probability, and if the probability of LCC openings has a major influence on the frequency of resting spark activity, then we should expect a reduced frequency of resting sparks in KO cells. It has been argued that spontaneous openings of RyRs, not LCC open probability, determine resting spark frequency (5). However, several studies support the idea that LCCs may influence resting spark frequency (34–36). Regardless of the mechanism of this interaction, it is plausible that the reduced LCC activity caused by relatively higher cleft Ca^{2+} reduces spontaneous Ca^{2+} sparks.

Although we did not test SR content under conditions identical to those used in this experiment, we have consistently found that SR Ca^{2+} is similar in patch-clamped WT and KO myocytes (16,19) This is also the case in the experiments shown in Figs. 3 and 4, where EGTA and/or fluo-3 were used to buffer Ca^{2+}. If there were any difference in SR content, we would have predicted that WT cells would be relatively depleted of Ca^{2+} compared with KO, since forward NCX in the WT cells would tend to remove Ca^{2+} under our experimental conditions (−75 mV holding potential and 10 mM Na^+ in the pipette). Of course, there is no NCX in KO cells to remove Ca^{2+}. A depleted SR in WT would not be consistent with the higher spark frequency we observed in WT compared to KO cells. Thus, we believe our results are not adequately explained by differences in SR load.

We have previously reported that in patch-clamped rabbit ventricular myocytes, resting spark frequency increases immediately when NCX is blocked abruptly by removing external Na^+ (in the absence of pipette Na^+) (20). How can we reconcile these results with those from the experiment shown in Fig. 1? We suggest that in rabbit cells, the abrupt removal of Na^+ to block NCX does not lead to a significant reduction in LCC activity. Instead, LCC activity remains steady and spark frequency increases, because the rise in cleft Ca^{2+} due to ongoing SR leak increases the probability of RyR triggering. In contrast, resting spark frequency in NCX KO is low despite relatively elevated ambient cleft Ca^{2+}, apparently because spark frequency is dominated by the reduced LCC activity caused by Ca^{2+}-induced inactivation (18).

How can we explain the difference in Ca^{2+} spark size in KO versus WT cells? The maximum size of a spark is determined by two basic processes, the rate at which Ca^{2+} is released to form the spark and the rate at which Ca^{2+} is removed from the vicinity of the spark. NCX falls into the latter category, and its absence in KO myocytes likely accounts for the greater amplitude and width of the spontaneous sparks.

In aggregate, these arguments support the importance of junctional microdomains in determining, among other things, the characteristics of spontaneous sparks. In particular, it seems likely to us that the extent to which a junctional microdomain is filled with Ca^{2+} will influence the likelihood that a spontaneous spark is activated by I_{Ca}, i.e., the coupling fidelity of I_{Ca} is increased by diadic cleft priming. We do not exclude the possibility that there are spontaneous openings of RyRs that produce sparks, particularly in nonjunctional RyRs, but our preliminary data suggest that their occurrence is low (N. Torres, F. Sachse, J. Goldhaber, and J. H. B. Bridge, unpublished observations).

Defective spark recruitment in NCX KO myocytes revealed by Ca^{2+} buffering

The fundamental unit of EC coupling in heart, the couplon, is composed of a cluster of LCCs in the sarcolemmal membrane of the t-tubule opposed to a cluster of RyRs on the SR membrane (3,37). Upon depolarization during an AP, LCCs in a couplon open and allow Ca^{2+} influx with consequent triggering of RyRs. RyRs are likely triggered by Ca^{2+} entering with the earliest opening of an LCC in a cluster that has a sufficient open time to deliver enough Ca^{2+} across the cleft (22,38). Since most LCC openings in response to depolarization occur with a short latency, they activate RyRs and produce sparks with a short latency (38). LCC openings with longer latencies also occur, but these are less frequent and ordinarily are obscured by the earlier openings within a cluster.

In NCX KO myocytes, there is a reduced number of Ca^{2+} sparks triggered with a short latency. There is also an increased number of temporally silent areas where triggering fails (Fig. 3 *B*, *arrows*). We found no evidence for structural changes in terms of t-tubule distribution (Fig. S1) that might explain the loss of spark production in NCX KO myocytes, though it is possible that 3-D reconstructions might reveal differences in t-tubular structure that we cannot appreciate in 2-D (39). However, we did observe that the extent of the reduction in early spark triggering was clearly influenced by the degree of Ca^{2+} buffering. Strong buffering (fluo-3 + EGTA) was associated with a more profound defect in triggering in KO compared to WT than weak buffering (fluo-3 alone). Since SR content is the same in KO and WT myocytes, and since our permeabilization experiments demonstrate that RyR function is similar in KO and WT myocytes, we must look to other processes for an explanation of spark failure in the KO myocytes.

In KO myocytes, Ca^{2+} is elevated in the subsarcolemmal space (18). Elevated subsarcolemmal Ca^{2+} promotes Ca^{2+}-dependent inactivation, thereby reducing the amount of

Ca^{2+} entering through LCCs (18) and reducing triggering of RyRs. However, this tendency is counteracted by two factors: 1), the more rapid repolarization of the AP in KO myocytes, which enhances coupling fidelity (19,40,41); and 2), the elevated cleft Ca^{2+}, which permits RyR triggering with less additional Ca^{2+} entry through LCCs. This means, in effect, that the increased Ca^{2+} in the cleft increases the coupling fidelity of I_{Ca}. Thus, in KO cells, the cleft space is already primed with Ca^{2+}, and RyRs are readily triggered by incremental increases in cleft-space Ca^{2+} by LCC openings. When we deplete Ca^{2+} in the cleft by including high concentrations of a Ca^{2+} chelator in the patch pipette, I_{Ca} likely returns to WT levels (18). However, this restored Ca^{2+} flux through LCCs cannot trigger RyRs with the same efficiency in the KO, because the diadic cleft space is no longer primed in the presence of EGTA. Thus, the recovery of I_{Ca} magnitude cannot overcome the lack of priming of the cleft with Ca^{2+}. As a consequence, in unbuffered KO cells, Ca^{2+} entering through LCCs is reduced, but paradoxically, it is more likely to trigger SR Ca^{2+} release because of the increased baseline cleft Ca^{2+}.

Why, then, are WT myocytes able to trigger calcium release even when the subsarcolemmal space is buffered with EGTA? We suggest that in WT cells, NCX operating in reverse mode primes the diadic cleft with Ca^{2+} upon depolarization, so that the incremental Ca^{2+} entering through LCCs can now trigger RyRs. It is well known that spikelike local release events can be elicited in the presence of EGTA (22,29,42), and even 10 mM EGTA cannot eliminate the influence of SR Ca^{2+} release on inactivation of I_{Ca} (43). We conclude that EGTA is too slow to prevent a transient accumulation of Ca^{2+} in the cleft produced by reverse NCX. We emphasize that the function of NCX here is to prime the cleft but not necessarily to directly trigger release. This effect of NCX is consistent with the close anatomical relationship between NCX, LCCs, and RyRs in the diadic cleft, as previously argued (15,44). We propose that the activity of NCX occurs immediately upon depolarization and proceeds with a latency that is significantly shorter than that exhibited by any Ca^{2+} channel. To summarize, in the absence of either elevated subsarcolemmal Ca^{2+} in the diadic cleft or reverse NCX to prime the diadic cleft with Ca^{2+}, LCCs by themselves are incapable of reliably triggering RyRs. Thus, couplon recruitment is less effective in KO myocytes buffered with EGTA, because cleft Ca^{2+} is low and the coupling fidelity of LCCs is also low. We cannot exclude the possibility that the shorter AP duration in KO myocytes compared to WT contributes to the reduced spark recruitment in EGTA. However, since the KO AP duration is the same in both the absence and presence of EGTA, the critical difference must be the coupling fidelity. The most likely mechanism for influencing the coupling fidelity is the extent to which the diadic cleft is primed with Ca^{2+}.

The mechanism we have outlined is intrinsically nonlinear. If we consider the sigmoid dependence of RyR open probability on gating Ca^{2+} concentration (45), the open probability at rest is set by the level of cleft Ca^{2+}. This resides at the far left of the sigmoid curve. Priming of the cleft by NCX might be expected to shift Ca^{2+} concentration along the flat portion of this sigmoid curve to its point of initial inflection, where we would not expect to see much increase in the open probability of RyRs. However, any further increase in cleft Ca^{2+} at the point of inflection would produce a rapid increase in the open probability of RyRs. In the absence of priming, Ca^{2+} channels will first have to elevate Ca^{2+} to the point of inflection before significant triggering will occur.

Origin of sparks with long latency

In WT rabbit myocytes, we have reported that the latencies of sparks triggered by depolarization reflect the latencies of LCC openings (22). The histograms in Figs. 3 and 4 show that activation of the late pool of sparks in KO myocytes occurs well after repolarization of the AP, when the open probability for LCCs is expected to be very low. It seems unlikely that these late Ca^{2+} sparks (occurring >30 ms after the stimulus) are triggered events that reflect the distribution of LCC open probability and open times. It is more likely that in the setting of slowed efflux due to the absence of NCX, Ca^{2+} released by RyRs within the first few milliseconds of the Ca^{2+} transient raises the concentration of Ca^{2+} in nearby diadic clefts to levels high enough for late sparks to be triggered by stochastic openings of LCCs. The probability of these sparks subsequently declines during the diastolic interval, presumably because the plasma membrane Ca^{2+} pump continues to reduce cleft Ca^{2+} during this period. Additional mechanisms, e.g., diffusion of Ca^{2+} out of the cleft and uptake of cytoplasmic Ca^{2+} by SERCA, also contribute to the decline of spark occurrence in diastole. Stochastic openings of RyRs (e.g., independent of LCCs) are unlikely to explain the late sparks. This is because the flux of Ca^{2+} passing through an RyR is significantly larger than that passing through an LCC and would therefore be expected to fill the cleft sufficiently to produce regenerative activation of a couplon even in the absence of cleft priming. The addition of 3 mM EGTA restricts Ca^{2+} diffusion and reduces priming of the diadic cleft by SR Ca^{2+}, which reduces the occurrence of late Ca^{2+} sparks by 70% compared to recordings in the absence of EGTA (Fig. 5).

When regarding the spatially averaged Ca^{2+} transient, late sparks contribute to its slowed relaxation in KO compared to WT cells (Fig. 6). The explanation for this slowed relaxation is the same as that given above for slowed efflux from the diadic cleft, and is primarily a consequence of the elimination of NCX. KO cells compensate for this reduced Ca^{2+} removal rate by reducing Ca^{2+} influx through an upregulation of I_{to} and a reduction in I_{Ca} (19).

CONCLUSIONS

We conclude that NCX is an essential component of the Ca^{2+} release trigger in cardiac myocytes. NCX activity ensures that the diadic cleft is primed with Ca^{2+} during an AP, and due to nonlinearities that are intrinsic to the entire trigger mechanism (46), produces disproportionately large effects of depolarization-induced openings of LCCs on RyR gating. Loss of NCX lowers EC coupling efficiency by reducing the coupling fidelity of LCCs and therefore the probability of couplon activation. Thus, reducing subsarcolemmal Ca^{2+} with EGTA in NCX KO mice reveals the dependence of Ca^{2+} release on NCX.

SUPPORTING MATERIAL

Methods, one figure, and additional references are available at http://www.biophysj.org/biophysj/supplemental/S0006-3495(10)00621-1.

The authors thank Scott T. Lamp for assistance with spark analysis.

This work was supported by National Institutes of Health grants R01HL70828 to J.I.G. and RO1HL4850 to K.D.P., American Heart Association Western States Affiliate grant GIA0755091Y to J.I.G., and by the Fulbright Program (P.N.).

REFERENCES

1. Fabiato, A. 1983. Calcium-induced release of calcium from the cardiac sarcoplasmic reticulum. *Am. J. Physiol.* 245:C1–C14.
2. Radermacher, M., V. Rao, …, T. Wagenknecht. 1994. Cryo-electron microscopy and three-dimensional reconstruction of the calcium release channel/ryanodine receptor from skeletal muscle. *J. Cell Biol.* 127:411–423.
3. Franzini-Armstrong, C., F. Protasi, and V. Ramesh. 1999. Shape, size, and distribution of Ca^{2+} release units and couplons in skeletal and cardiac muscles. *Biophys. J.* 77:1528–1539.
4. Izu, L. T., and C. W. Balke. 2002. The Ca^{2+} synapse redo: a matter of location, location, location. *Circ. Res.* 91:276–277.
5. Cheng, H., W. J. Lederer, and M. B. Canneldl. 1993. Calcium sparks: elementary events underlying excitation-contraction coupling in heart muscle. *Science.* 262:740–744.
6. Lopez-Lopez, J. R., P. S. Shacklock, …, W. G. Wier. 1995. Local calcium transients triggered by single L-type calcium channel currents in cardiac cells. *Science.* 268:1042–1045.
7. LeBlanc, N., and J. R. Hume. 1990. Sodium current-induced release of calcium from cardiac sarcoplasmic reticulum. *Science.* 248:372–376.
8. Lines, G. T., J. B. Sande, …, O. M. Sejersted. 2006. Contribution of the Na^+/Ca^{2+} exchanger to rapid Ca^{2+} release in cardiomyocytes. *Biophys. J.* 91:779–792.
9. Litwin, S. E., J. Li, and J. H. Bridge. 1998. Na-Ca exchange and the trigger for sarcoplasmic reticulum Ca release: studies in adult rabbit ventricular myocytes. *Biophys. J.* 75:359–371.
10. Wasserstrom, J. A., and A. M. Vites. 1996. The role of Na^+-Ca^{2+} exchange in activation of excitation-contraction coupling in rat ventricular myocytes. *J. Physiol.* 493:529–542.
11. Han, C., P. Tavi, and M. Weckstrom. 2002. Role of the Na^+-Ca^{2+} exchanger as an alternative trigger of CICR in mammalian cardiac myocytes. *Biophys. J.* 82:1483–1496.
12. Näbauer, M., G. Callewaert, …, Morad. 1989. Regulation of calcium release is gated by calcium current, not gating charge, in cardiac myocytes. *Science.* 244:800–803.
13. Sham, J. S., L. Cleemann, and M. Morad. 1992. Gating of the cardiac Ca^{2+} release channel: the role of Na^+ current and Na^+-Ca^{2+} exchange. *Science.* 255:850–853.
14. Sipido, K. R., M. Maes, and F. Van de Werf. 1997. Low efficiency of Ca^{2+} entry through the Na^+-Ca^{2+} exchanger as trigger for Ca^{2+} release from the sarcoplasmic reticulum. A comparison between L-type Ca^{2+} current and reverse-mode Na^+-Ca^{2+} exchange. *Circ. Res.* 81:1034–1044.
15. Thomas, M. J., I. Sjaastad, …, O. P. Ottersen. 2003. Localization and function of the Na^+/Ca^{2+}-exchanger in normal and detubulated rat cardiomyocytes. *J. Mol. Cell. Cardiol.* 35:1325–1337.
16. Henderson, S. A., J. I. Goldhaber, …, K. D. Philipson. 2004. Functional adult myocardium in the absence of Na^+-Ca^{2+} exchange: cardiac-specific knockout of NCX1. *Circ. Res.* 95:604–611.
17. Pott, C., X. Ren, …, J. I. Goldhaber. 2007. Mechanism of shortened action potential duration in Na^+-Ca^{2+} exchanger knockout mice. *Am. J. Physiol. Cell Physiol.* 292:C968–C973.
18. Pott, C., M. Yip, …, K. D. Philipson. 2007. Regulation of cardiac L-type Ca^{2+} current in Na^+-Ca^{2+} exchanger knockout mice: functional coupling of the Ca^{2+} channel and the Na^+-Ca^{2+} exchanger. *Biophys. J.* 92:1431–1437.
19. Pott, C., K. D. Philipson, and J. I. Goldhaber. 2005. Excitation-contraction coupling in Na^+-Ca^{2+} exchanger knockout mice: reduced transsarcolemmal Ca^{2+} flux. *Circ. Res.* 97:1288–1295.
20. Goldhaber, J. I., S. T. Lamp, …, J. N. Weiss. 1999. Local regulation of the threshold for calcium sparks in rat ventricular myocytes: role of sodium-calcium exchange. *J. Physiol.* 520:431–438.
21. Zima, A. V., J. Kockskamper, and L. A. Blatter. 2006. Cytosolic energy reserves determine the effect of glycolytic sugar phosphates on sarcoplasmic reticulum Ca^{2+} release in cat ventricular myocytes. *J. Physiol.* 577:281–293.
22. Chantawansri, C., N. Huynh, …, J. I. Goldhaber. 2008. Effect of metabolic inhibition on couplon behavior in rabbit ventricular myocytes. *Biophys. J.* 94:1656–1666.
23. Wang, S. Q., L. S. Song, …, H. Cheng. 2001. Ca^{2+} signalling between single L-type Ca^{2+} channels and ryanodine receptors in heart cells. *Nature.* 410:592–596.
24. Neher, E. 1998. Vesicle pools and Ca^{2+} microdomains: new tools for understanding their roles in neurotransmitter release. *Neuron.* 20:389–399.
25. Pape, P. C., D. S. Jong, and W. K. Chandler. 1995. Calcium release and its voltage dependence in frog cut muscle fibers equilibrated with 20 mM EGTA. *J. Gen. Physiol.* 106:259–336.
26. Song, L. S., J. S. Sham, …, H. Cheng. 1998. Direct measurement of SR release flux by tracking "Ca^{2+} spikes" in rat cardiac myocytes. *J. Physiol.* 512:677–691.
27. Gómez, J., P. Neco, …, J. L. Vergara. 2006. Calcium release domains in mammalian skeletal muscle studied with two-photon imaging and spot detection techniques. *J. Gen. Physiol.* 127:623–637.
28. Zahradnikova, Jr., A., E. Polakova, …, A. Zahradnikova. 2007. Kinetics of calcium spikes in rat cardiac myocytes. *J. Physiol.* 578:677–691.
29. Cleemann, L., W. Wang, and M. Morad. 1998. Two-dimensional confocal images of organization, density, and gating of focal Ca^{2+} release sites in rat cardiac myocytes. *Proc. Natl. Acad. Sci. USA.* 95:10984–10989.
30. Escobar, A. L., F. Cifuentes, and J. L. Vergara. 1995. Detection of Ca^{2+}-transients elicited by flash photolysis of DM-nitrophen with a fast calcium indicator. *FEBS Lett.* 364:335–338.
31. He, J., M. W. Conklin, …, T. J. Kamp. 2001. Reduction in density of transverse tubules and L-type Ca^{2+} channels in canine tachycardia-induced heart failure. *Cardiovasc. Res.* 49:298–307.
32. Louch, W. E., B. Vito, …, K. R. Sipido. 2004. Reduced synchrony of Ca^{2+} release with loss of T-tubules: a comparison to Ca^{2+} release in human failing cardiomyocytes. *Cardiovasc. Res.* 62:63–73.

33. Song, L. S., E. S. Sobie, …, H. Cheng. 2006. Orphaned ryanodine receptors in the failing heart. *Proc. Natl. Acad. Sci. USA*. 103: 4305–4310.

34. Copello, J. A., A. V. Zima, …, L. A. Blatter. 2007. Ca^{2+} entry-independent effects of L-type Ca^{2+} channel modulators on Ca^{2+} sparks in ventricular myocytes. *Am. J. Physiol. Cell Physiol.* 292:C2129–C2140.

35. Satoh, H., H. Katoh, …, D. M. Bers. 1998. Bay K 8644 increases resting Ca^{2+} spark frequency in ferret ventricular myocytes independent of Ca influx: contrast with caffeine and ryanodine effects. *Circ. Res.* 83:1192–1204.

36. Sheehan, K. A., A. V. Zima, and L. A. Blatter. 2006. Regional differences in spontaneous Ca^{2+} spark activity and regulation in cat atrial myocytes. *J. Physiol.* 572:799–809.

37. Stern, M. D. 1992. Theory of excitation-contraction coupling in cardiac muscle. *Biophys. J.* 63:497–517.

38. Inoue, M., and J. H. Bridge. 2003. Ca^{2+} sparks in rabbit ventricular myocytes evoked by action potentials: involvement of clusters of L-type Ca^{2+} channels. *Circ. Res.* 92:532–538.

39. Savio-Galimberti, E., J. I. Goldhaber, …, F. B. Sachse. 2007. A framework for analyzing confocal images of transversal tubules in cardiomyocytes. *In* Functional Imaging and Modeling of the Heart.. Springer, Berlin. 110–119.

40. Sah, R., R. J. Ramirez, and P. H. Backx. 2002. Modulation of Ca^{2+} release in cardiac myocytes by changes in repolarization rate: role of phase-1 action potential repolarization in excitation-contraction coupling. *Circ. Res.* 90:165–173.

41. Zahradnikova, A., Z. Kubalova, …, I. Zahradnik. 2004. Activation of calcium release assessed by calcium release-induced inactivation of calcium current in rat cardiac myocytes. *Am. J. Physiol. Cell Physiol.* 286:C330–C341.

42. Fukumoto, G. H., S. T. Lamp, …, J. I. Goldhaber. 2005. Metabolic inhibition alters subcellular calcium release patterns in rat ventricular myocytes: implications for defective excitation-contraction coupling during cardiac ischemia and failure. *Circ. Res.* 96:551–557.

43. Sham, J. S., L. Cleemann, and M. Morad. 1995. Functional coupling of Ca^{2+} channels and ryanodine receptors in cardiac myocytes. *Proc. Natl. Acad. Sci. USA*. 92:121–125.

44. Peskoff, A., and G. A. Langer. 1998. Calcium concentration and movement in the ventricular cardiac cell during an excitation-contraction cycle. *Biophys. J.* 74:153–174.

45. Copello, J. A., S. Barg, …, S. Fleischer. 1997. Heterogeneity of Ca^{2+} gating of skeletal muscle and cardiac ryanodine receptors. *Biophys. J.* 73:141–156.

46. Zahradnikova, A., M. Dura, …, S. Gyorke. 2003. Regulation of dynamic behavior of cardiac ryanodine receptor by Mg^{2+} under simulated physiological conditions. *Am. J. Physiol. Cell Physiol.* 285:C1059–C1070.